Since, as discussed above, $Fe(CN)_6^{3-}$ does not diffuse across the vesicle membrane over the time course of these studies, the rate behavior implies net transmembrane redox involving the bound viologens. Reaction mechanisms could involve either transmembrane diffusion of $C_{16}MV^+$ from the outer to inner surface or transmembrane electron exchange between external $C_{16}MV^+$ and internal $C_{16}MV^{2+}$ ions, followed by radical scavenging by $Fe(CN)_6^{3-}$ on the inner surface. Asymmetrically organized vesicles with $C_{16}MV^{2+}$ only bound to their outer surfaces and carrying internaized $Fe(CN)_6^{3-}$ showed immediate formation of viologen radical, i.e., no induction, with a 5-fold rate enhancement over the photosensitized reaction in absence of $Fe(CN)_6^{3-}$. Thus, the transmembrane reaction requires $C_{16}MV^{2+}$ on both surfaces, an observation that is most simply interpreted in terms of transmembrane electron exchange between the viologen mono- and dications. Rate parameters determined from initial slopes of absorbance vs. time plots for $C_{16}MV^{2+}$ reduction in various vesicle configurations are listed in Table II. Studies are continuing to identify the transmembrane oxidation-reduction mechanism.

Concluding Remarks

Adsorption of $Zn(TMPyP)^{4+}$ ion onto DHP vesicles generates a multiplicity of deactivation pathways for the photoexcited ion. Three predominant pathways involving self-quenching, ionogenesis, and "spontaneous" decay have been identified from observation of the kinetic and optical absorption properties of the transient species and their reactivities toward alkylviologens. Although this mechanistic diversity implies the existence of molecular organizates at the vesicle interface, we could find no evidence for aggregation using absorption spectrophotometric methods. The rapid formation of Zn(II) porphyrin π-ions is particularly noteworthy since they may arise by oxidation-reduction involving singlet photoexcited ions. In this sense, the reaction may mimic photosynthetic redox centers, for which charge separation is initiated from photoexcited singlet states.[52,53] In vitro models exhibiting detectable charge pair formation emanating from the singlet state are rare; most examples are covalently linked photoredox pairs that meet special spatial and orientational geometric requirements.[54]

The inefficient formation of redox products by oxidative quenching when both $Zn(TMPyP)^{4+}$ and acceptor viologens are adsorbed to the vesicle is a consequence of a relatively slow reaction between bound reactants (eq 4), rapid cyclic back electron transfer from π-anion to π-cation using viologen as the relay (eq 2, 3), and, at higher surface concentrations, competitive self-quenching of the sensitizer triplet ion. The relative rates can be rationalized by assuming that the monopositively charged viologen radicals have relatively large mobilities on the vesicle surface, presumably because electrostatic forces are considerably less than for the other ions. This might be interpreted as weaker Coulombic attraction or binding at a single surface site, as opposed to formation of two and four distinct electrostatic bonds upon adsorption of C_nMV^{2+} and $Zn(TMPyP)^{4+}$ ions, respectively. Since the diffusional barrier for $Zn(TMPyP)^{3+}$ ion is overcome by its release from DHP, both reactions 2 and 3 involve relatively mobile species whereas reaction 4 does not.

Regardless of mechanistic interpretations, it is evident that vesicles and liposomal suspensions are capable of dramatically altering the solution photochemistry of Zn(II) porphyrins. The most useful observation from the standpoint of photoconversion is that selective adsorption of viologens to DHP provides a means for overcoming static quenching that otherwise occurs by $Zn(TPPS)^{4-}$-C_nMV^{2+} ion pair formation and severely limits net redox in homogeneous solution. Use of DHP in this instance is particularly effective because the electrostatic barrier imposed by the anionic vesicle surface to electron transfer across the aqueous-vesicle interface is small (e.g., k_Q for oxidative quenching of $^3(Zn(TPPS)^{4-})$ by MV^{2+} and MV^{2+}-DHP are 1.4×10^{10} M^{-1} s^{-1} (ref 28) and 2.5×10^9 M^{-1} s^{-1}, respectively). In general, since bound viologen appears to act as a transmembrane charge relay and $Zn(TMPyP)^{4+}$ binding leads to its own destabilization, systems containing Zn(II) porphyrins in solution with membrane-bound acceptors will be more practicable than other spatial configurations in application to photocatalytic devices that rely upon generation of membrane separated redox products.

Acknowledgment. J.K.H. and L.Y.C.L. express their gratitude to Drs. Andrê M. Braun and Kuppuswamy Kalyanasundaram, EPFL, for their generous gifts of experimental materials, to Drs. Robin Humphry-Baker, Pierre P. Infelta, and Keith Monserrat, EPFL, for instruction and advice on experimental methodology, and to Dr. Yves-M. Tricot, CSIRO, for communicating results prior to publication. Financial support was provided by the Oregon Graduate Center through the auspices of its faculty sabbatical leave program and by NIH through a grant (GM 20943) to J.K.H.

Registry No. $Zn(TMPy)^{4+}$, 40603-58-5; $Zn(TPPS)^{4-}$, 80004-36-0; $C_{14}MV^{2+}$, 79039-57-9; $C_{16}MV^{2+}$, 77814-50-7; MV^{2+}, 4685-14-7; $Fe(CN)_6^{3-}$, 13408-62-3; DHP, 2197-63-9.

(52) Shuvalov, V. A.; Parson, W. W. *Proc. Natl. Acad. Sci. U.S.A.* **1981**, *78*, 957-961, and references therein.
(53) Shuvalov, V. A.; Klevanik, A. V.; Sharkov, A. V.; Kryukov, P. G.; Ke, B. *FEBS Lett.* **1979**, *107*, 313-316.
(54) Connolly, J. S. In "Photochemical Conversion and Storage of Solar Energy—1982", Part A; Rabani, J., Ed.; Weizmann Science Press of Israel: 1982; pp 175-204, and references therein.

The Absence of Bonding Electron Density in Certain Covalent Bonds As Revealed by X-ray Analysis

Jack D. Dunitz* and Paul Seiler

Contribution from the Organic Chemistry Laboratory of the Swiss Federal Institute of Technology, CH-8092 Zürich, Switzerland. *Received May 18, 1983*

Abstract: Electron-density difference maps obtained from an accurate low-temperature X-ray analysis of 1,2,7,8-tetraaza-4,5,10,11-tetraoxatricyclo[6.4.1.1^{2,7}] tetradecane (**1**) show a density deficit at the center of the O-O bond and only weak density accumulations at the centers of the C-O and N-N bonds. Peaks corresponding to tetrahedrally oriented lone pairs are observed at the N and O atoms. These findings and others indicate that accumulation of charge (bonding density) in the internuclear region as occurs in the hydrogen molecule may not be characteristic of covalent bonds in general.

Because of its relative simplicity, the H_2 molecule is generally taken as the paradigm of the covalent bond,[1] and one of its cardinal features, the accumulation of negative charge between the nuclei, seems to have established itself as the standard textbook expla-

0002-7863/83/1505-7056$01.50/0

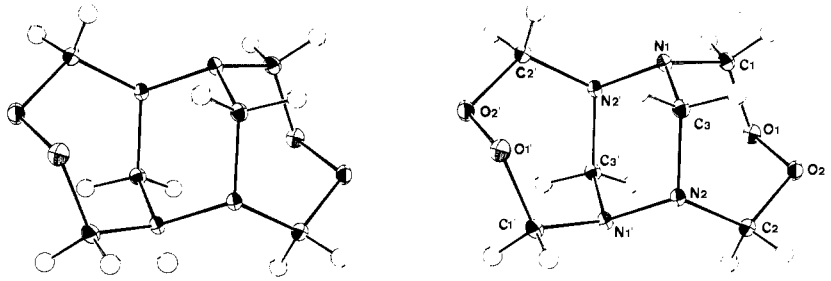

Figure 1. Stereoscopic view of molecule **1** with vibration ellipsoids (50% probability level) and atomic numbering.

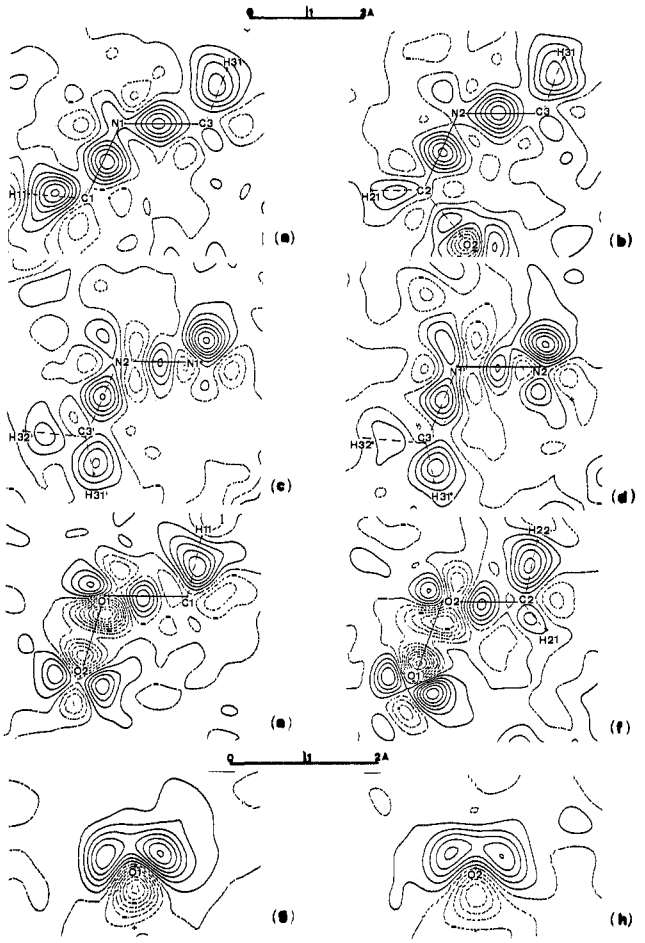

Figure 2. Several sections through the electron-density difference map (for atom numbering see Figure 1). The planes shown are through the following: (a) C1,N1,C3; (b) C2,N2,C3; (c) N2′,N1, and the midpoint of C1 and C3; (d) N1′,N2, and the midpoint of C_2 and C3; (e) O2,O1,C1; (f) O1,O2,C2; (g) perpendicular to e and passing through O1 and the midpoint of O2 and C1; (h) perpendicular to f and passing through O2 and the midpoint of O1 and C2. Bonds indicated by dashed lines do not lie in the defined planes. Contour lines are drawn at intervals of 0.075 e·Å^{-3}, full for positive, dashed for negative, and dotted for zero density. The standard deviation of the difference density estimated as $[2\Sigma\sigma^2(F_o)]^{1/2}/V$ is 0.013 e·Å^{-3}.

nation of the phenomenon of chemical bonding in general.

During recent years, the charge distribution in molecular crystals has become increasingly amenable to experimental study by means of electron-density difference maps from X-ray analysis.[3,4] Such maps typically show "bonding density" peaks at or near the expected positions between formally bonded atoms, but there are notable exceptions.[5]

We have now made a study of the difference density in 1,2,7,8-tetraaza-4,5,10,11-tetraoxatricyclo[6.4.1.1^{2,7}]tetradecane (**1**)[8] from an X-ray analysis based on extensive low-temperature

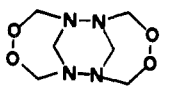

(**1**)

(96 K) measurements.[11] Figure 1 shows a stereoview of **1**, which sits at a site of inversion symmetry in the crystal. Bond lengths are within 0.005 Å of those published previously,[10] and bond angles are within 0.5.[15] Figure 2 shows sections of the final electron-

(1) Attempts[2] to understand the underlying physical mechanism of the covalent bond have actually tended to concentrate on the H_2^+ ion (one-electron bond) and to generalize the conclusions with minor modifications to cover the H_2 molecule (electron-pair bond). There the matter has usually been left, either because the problem was regarded as being essentially solved or possibly because the extrapolation to many-electron systems was recognized as involving far-reaching complications.

(2) Notably: (a) Ruedenberg, K. *Rev. Mod. Phys.* **1962**, *34*, 326–376. (b) Kutzelnigg, W. *Angew. Chem.* **1973**, *85*, 551–568; *Angew. Chem., Int. Ed. Engl.* **1973**, *12*, 546–562.

(3) See: Dunitz, J. D. "X-ray Analysis and the Structure of Organic Molecules"; Cornell University Press; Ithaca, N.Y., 1979; Chapter 8.

(4) (a) Hirshfeld, F. L., Ed. *Isr. J. Chem.* **1977**, *16*, 87–229. (b) Becker, P., Ed. "Electron and Magnetization Densities in Molecules and Crystals"; Plenum Press: New York, 1980. (c) Coppens, P.; Hall, M. B., Eds. "Electron Distributions and the Chemical Bond"; Plenum Press: New York, 1982.

(5) No bonding density is observed for the bond between the inverted C atoms in a [3.1.1]propellane derivative,[6] in agreement with results of theoretical calculations for [1.1.1]propellane.[7]

(6) Chakrabarti, P.; Seiler, P.; Dunitz, J. D.; Schlüter, A.-D.; Szeimies, G. *J. Am. Chem. Soc.* **1981**, *103*, 7378–7380.

(7) (a) Newton, M. D.; Schulman, J. M. *J. Am. Chem. Soc.* **1972**, *94*, 773–778. (b) Bader, R. F. W.; Tang, T. H.; Tal, Y.; Biegler-König. *Ibid.* **1982**, *104*, 940–945. (c) Wiberg, K. B. *Ibid.* **1983**, *105*, 1227–1233.

(8) Obtained by the reaction of hydrazine with formaldehyde in the presence of hydrogen peroxide.[9] The identity of the colorless crystalline product was established as **1** by X-ray analysis.[10]

(9) von Giersewald, C.; Silgens, H. *Ber. Dtsch. Chem. Ges.* **1921**, *54*, 492–497.

(10) Whittleton, S. N.; Seiler, P.; Dunitz, J. D. *Helv. Chim. Acta* **1981**, *64*, 2614–2616.

(11) Colorless crystals of $C_6H_{12}N_4O_4$ are triclinic, space group $P\bar{1}$, cell dimensions a = 6.068, b = 6.139, c = 6.579 Å, α = 105.99°, β = 102.55°, γ = 112.75° at 96 K (compare ref 10), Z = 1. Intensity measurements were made with a Enraf-Nonius CAD-4 diffractometer equipped with graphite monochromator (Mo Kα radiation) and cooling device. Because of radiation damage, two crystals were measured: crystal A, 2496 independent reflections out to $(\sin\theta)/\lambda$ = 0.905 Å^{-1} [2178 with $I > 3\ \sigma(I)$]; crystal B, 6103 independent reflections out to $(\sin\theta)/\lambda$ = 1.22 Å^{-1} [4612 with $I > 3\sigma(I)$]. The difference maps shown in Figure 2 are calculated with 2191 $(F_o - F_c)$ coefficients from crystal A with $\sin\theta/\lambda < 0.905$ Å^{-1} and $F_o \geq 5\sigma(F_o)$ with F_c calculated from atomic coordinates and vibration parameters obtained by full-matrix least-squares analysis of 2249 high-order F values with $\sin\theta/\lambda > 0.905$ Å^{-1} and $F_o \geq 10\sigma(F_o)$ from crystal B (R = 0.013) using the XRAY system.[12] Atomic scattering factors for C, N, O were taken from ref 13 and for H from ref 14. For the F_c calculation, H atoms were displaced from their refined positions along the appropriate C–H directions to a C–H distance of 1.08 Å. An extinction correction was applied to the low-order data from crystal A. It was estimated by holding all other parameters constant, except the scale factor. The problems of optimally combining two data sets, each involving different degrees of radiation damage, are not trivial, and full details will be reported elsewhere. A table of atomic coordinates and vibration parameters is provided as supplementary material.

(12) Stewart, J. M.; Kruger, G. J.; Ammon, H. L., Dickinson, C.; Hall, S. R. "The XRAY System; version of June 1972"; Technical Report TR 192, Computer Science Center, University of Maryland, College Park, MD.

(13) Cromer, D. T.; Mann, J. B. *Acta Crystallogr., Sect. A* **1968**, *24A*, 321–324.

(14) Stewart, R. F.; Davidson, E. R.; Simpson, W. T. *J. Chem. Phys.* **1965**, *42*, 3175–3187.

density difference maps through various planes of interest. These maps portray the difference between the actual electron density in the unit cell of the crystal and the superposition of the spherically averaged free-atom densities, in other words, the change in electron density associated with molecule formation from free atoms.[16]

Figure 2 shows that this deformation density is different for the different kinds of bond in the molecule; it decreases in the order C–N > C–O > N–N > O–O.[17] The density along the O–O bond is seen to be negative throughout; there are two deep troughs of about −0.4 to −0.55 e·Å^{-3} separated by a central maximum that rises to about −0.05 e·Å^{3}. The density along the N–N bond is also mainly negative but rises to a central maximum of about +0.22 e·Å^{-3}. In contrast, the density peaks associated with the lone pairs of the N atoms reach heights of approximately +0.5 e·Å^{-3}, and those associated with the lone pairs of the O atoms are about +0.4 to +0.5 e·Å^{-3}, slightly higher than the peaks near the centers of the C–N bonds and nearly double those near the centers of the C–O bonds.[18]

The absolute values of these density peaks and troughs are not especially significant since they depend on details of the experiment and the refinement procedure.[19] However, the qualitative comparisons of these features of the various bonds and lone pairs in this molecule should be fairly reliable.

The relative weakness of the bonding density in C–O bonds compared with C–C bonds was apparent from previous X-ray studies of *trans*-2,5-dimethyl-3-hexene-2,5-diol hemihydrate at 86 K[20] and of 1,4,7,10,13,16-hexaoxacyclooctadecane (18-crown-6) at 100 K.[21] Similarly, the low bonding density in N–N bonds has been noted from studies of *N,N'*-diformylhydrazine,[22] tetraformylhydrazine,[23] and carbonohydrazide.[24] Only weak or even slightly negative bonding density has been found for the N–O bonds in 4-nitropyridine *N*-oxide[25] and uronium nitrate,[26] while a very recent study of the difference density in tetrafluoroterephthalonitrile[27] and 1,1,4,4-tetrafluorocyclohexane[27,28] has revealed the presence of only marginally positive maxima at the centers of C–F bonds. Likewise, difference maps for hydrogen peroxide based on X-ray and neutron diffraction measurements[19b] show negative bonding density in the O–O bond, quite similar to that found in the present investigation. Thus, our new results agree very nicely with previous observations but may be regarded as being somewhat more persuasive, since the presence of C–N, C–O, N–N, and O–O bonds in one and the same molecule ensures that certain types of error, which could otherwise vary from one crystal structure analysis to another, do not affect the comparisons.

The negative difference density along the O–O bond direction says that the total charge density along this line is *less* than the sum of the densities of spherically averaged ground-state oxygen atoms at the same nuclear positions, a result that seems to contradict the conventional view that a buildup of charge between the nuclei is necessary for covalent chemical bonding.

However, this need not come as a complete surprise since, according to calculated difference maps[29] based on Hartree–Fock charge distributions, only Li_2 among second-row homonuclear diatomic molecules fits the conventional picture of removal of charge from the antibonding regions and a buildup in the binding region. For the other homonuclear diatomics the binding region is increasingly depleted of charge density as we go toward F_2. In fact, the difference density we find for the O–O bond is remarkably similar to that calculated[29] for the F_2 molecule,[30] and the resemblance would be even closer if the calculated map were based on subtraction of spherically averaged densities for F atoms in their ground state instead of densities corresponding to atoms in a prepared valence state.[31]

The charge deficit in the bond region between electron-rich atoms can be attributed to the exclusion principle, which obviously, for these atoms, works against excessive accumulation of electron density in this region and hence against chemical bonding. On the other hand, according to calculations by Hirshfeld and Rzotkiewicz,[32] the classical interaction of two spherically averaged ground-state atomic charge distributions is always binding, and, indeed, for the second-row homonuclear diatomics, the classical pro-molecule is electrostatically considerably more stable than the actual molecule. The H_2 molecule with its two electrons is the only exception to this rule; here the pro-molecule is much less stable than the actual molecule. The very simplicity of the H_2 molecule, its solitary electron pair, makes it atypical, so that this molecule, far from being the paradigm, may not after all provide a good basis for the discussion of chemical bonding in general.[33]

Registry No. 1, 81286-97-7; hydrogen, 1333-74-0.

Supplementary Material Available: Table of positional and vibrational parameters (1 page). Ordering information is given on any current masthead page.

(15) Except that in ref 10 the bond angle at C2 was erroneously given as 111.5° instead of 115.5°.

(16) The free-atom densities are convoluted with the appropriate trivariate Gaussian functions (anisotropic vibrational parameters) to allow for thermal smearing. Static deformation density maps can also be obtained by expressing the deformation density in parametric form and refining the parameters, along with the usual positional and vibrational parameters, by least-squares analysis. See: Hirshfeld, F. L. *Acta Crystallogr., Sect. B* **1971**, *27B*, 769–781; *Isr. J. Chem.* **1977**, *16*, 168–174; Stewart, R. F. *Ibid.* **1977**, *16*, 124–131.

(17) Slight differences between the N1–C1 and N2–C2 bonds and between the C1–O1 and C2–O2 bonds may be associated with stereoelectronic factors. See ref 10.

(18) The distributions corresponding to oxygen lone pairs (Figure 2g,h) show two distinct peaks at about 0.4 Å from each atomic center, and making an angle of about 120–130°. The nitrogen lone pair peaks (Figure 2c,d) are also about 0.4 Å from the atomic centers. Notice the secondary lobes that appear opposite the lone pair peaks.

(19) See, for example: (a) Stevens, E. D.; Coppens, P. *Acta Crystallogr., Sect. B* **1980**, *36B*, 1864–1876. (b) Savariault, J. M.; Lehmann, M. S. *J. Am. Chem. Soc.* **1980**, *102*, 1298–1303.

(20) van der Wal, H. R.; Vos, A. *Acta Crystallogr., Sect. B* **1979**, *35B*, 1804–1809.

(21) Maverick, E.; Seiler, P.; Schweizer, W. B.; Dunitz, J. D. *Acta Crystallogr., Sect. B* **1980**, *36B*, 615–620.

(22) Hope, H.; Otterson, T. *Acta Crystallogr., Sect. B* **1979**, *35B*, 370–372.

(23) Otterson, T.; Almlöf, J.; Carle, J. *Acta Chem. Scand., Sect. A* **1982**, *36A*, 63–68.

(24) Otterson, T.; Hope, H. *Acta Crystallogr., Sect. B* **1979**, *35B*, 373–378.

(25) Wang, Y.; Blessing, R. H.; Ross, F. K.; Coppens, P. *Acta Crystallogr., Sect. B* **1976**, *32B*, 572–578. Coppens, P.; Lehmann, M. S. *Ibid.* **1976**, *32B*, 1777–1784.

(26) De With, G.; Harkema, S.; Feil, D. *Acta Crystallogr., Sect. A* **1975**, *31A*, 227–228. A theoretical difference map for the nitrate ion based on double-ζ HFS calculations also fails to show any bonding density in the N–O bonds.

(27) Dunitz, J. D.; Schweizer, W. B.; Seiler, P. *Helv. Chim. Acta* **1983**, *66*, 123–133.

(28) Dunitz, J. D.; Schweizer, W. B.; Seiler, P. *Helv. Chim. Acta* **1983**, *66*, 134–137.

(29) Bader, R. F. W.; Henneker, W. H.; Cade, P. E. *J. Chem. Phys.* **1967**, *46*, 3341–3363. See particularly Figure 3 of this paper.

(30) The calculated difference map for F_2 in Figure 3 of ref 29 is for stationary nuclei and shows a slightly positive central peak surrounded by deep negative regions. Convolution of this distribution with a Gaussian to simulate the effect of vibration must reduce the height of the central peak and broaden the troughs. Both kinds of change would make the calculated map even more similar to the experimental result for the O–O bond.

(31) The use of spherically averaged ground-state charge densities for the atoms constituting the pro-molecule may be questioned. However, this is the only choice that allows fully for the reduction in symmetry that occurs when the free atom becomes part of a molecule.

(32) Hirshfeld, F. L.; Rzotkiewicz, M. *Mol. Phys.* **1974**, *27*, 1319–1343.

(33) The atypical nature of the H_2 molecule and its unsuitability for a general discussion of the chemical bond are stressed by Hirshfeld and Rzotkiewicz.[32] See also footnote 20 of Bader and Beddall: Bader, R. F. W.; Beddall, P. M. *J. Chem. Phys.* **1972**, *56*, 3320–3329.